

Benchmarking quantum chemistry methods for spin-state energetics of iron complexes against quantitative experimental data

Electronic Supplementary Information (ESI)

Mariusz Radoń

E-mail: mradon@chemia.uj.edu.pl

In PDF format (this ESI document):

- additional tables with computational results
- additional figures
- complete refs 74, 75, 78, 80, 84, and 89
- additional references (S1-S12) to the basis sets

In TXT format (the other ESI document):

- Cartesian coordinates

Additional supporting data (structures and total energies from selected calculations)
may be accessed as an ioChem-BD collection under the following link:

<https://doi.org/10.19061/iochem-bd-7-1>

Table S1: Zero Point Energies (ZPE) and Vibrational Corrections ($\Delta H - \Delta E_e$ including ZPE) to Spin-State Energetics for SCO Complexes **3** and **4**.^a

model	ZPE (a.u.)		$\Delta H - \Delta E_e$ (kcal/mol)		ΔZPE (kcal/mol)	$\Delta[\Delta H - \Delta E_e]$ (kcal/mol)
	(S ₁)	(S ₂)	(S ₁)	(S ₂)		
3	0.44595	0.44226	296.4	295.5	-2.3	-0.9
4	0.42983	0.42602	276.7	274.9	-2.4	-1.7

^a Based on DFT:BP86-D3/def2-TZVP geometries and unscaled, gas-phase harmonic frequencies, computed with Turbomole. Temperature of $T(1/2) = \Delta H / \Delta S$ (from experimental values), i.e., 335 K for **3**, 192 K for **4**, was assumed for calculation of ΔH corrections.

Table S2: Symmetries of Electronic States and Occupations.

model	symmetry ^a	state	doubly occupied per irrep ^b	singly occupied per irrep ^b
1	D _{2h}	⁶ A _g	12,2,2,2,0,7,7,7	2,1,1,1,0,0,0,0
		⁴ B _{1g} ^c	12,3,2,2,0,7,7,7	1,0,1,1,0,0,0,0
		⁴ B _{2g} ^c	12,2,3,2,0,7,7,7	1,1,0,1,0,0,0,0
		⁴ B _{3g} ^c	12,2,2,3,0,7,7,7	1,1,1,0,0,0,0,0
2	C ₂	² A	32,30	1,0
		⁴ B	32,29	2,1
3	C ₂	¹ A	43,41	0,0
		⁵ B	41,41	3,1
4'	C ₂	² A	41,39	1,0
		⁶ A	40,38	3,2
4	C ₂	² A	49,47	1,0
		⁶ A	48,46	3,2

^a For **1** and **2** the highest Abelian subgroup. ^b Irreducible representations (irreps) are ordered as follows: a,b for C₂; a_g,b_{1g},b_{2g},b_{3g},a_u,b_{1u},b_{2u},b_{3u} for D_{2h}. ^c The three states are exactly degenerate as being components of the ⁴T_g state (under the true symmetry T_h).

Table S3: Estimating Solvation Effects for Spin-State Energetics of **3**.

	Total energies (a.u.) ^a		ΔE (kcal/mol)
	S=0	S=2	
gas/gas ^b	-2067.778703	-2067.752043	16.7
water/gas ^c	-2068.023362	-2067.992370	19.4
gas/water ^d	-2067.778091	-2067.751343	16.8
water/water ^e	-2068.023789	-2067.992726	19.5
3+6W , water/water ^{f, e}	-2526.961060	-2526.929565	19.8
		correction ^g	2.8

^a BP86-D3/def2-TZVP total energies from Turbomole calculations. ^b Energy calculations in gas phase for geometry optimized in gas phase; ^c Energy calculations in water (COSMO model, $\epsilon=80$) for geometry optimized in gas phase; ^d Energy calculations in gas phase for geometry optimized in water (COSMO model). ^e Energy calculations in water for geometry optimized in water (COSMO model $\epsilon=80$). ^f For model with added 6 explicit water molecules. ^g Difference between the ΔE values for solvated (water/water) and unsolvated (gas/gas) model, the values subtracted are boldfaced.

Table S4: Estimating Solvation Effects for for Spin-State Energetics of **4**.

	Total energies (a.u.) ^a		ΔE (kcal/mol)
	S=1/2	S=5/2	
gas/gas ^b	-2260.390305	-2260.364394	16.3
acetone/gas ^c	-2260.454079	-2260.427320	16.8
gas/acetone ^d	-2260.389648	-2260.363437	16.4
acetone/acetone ^e	-2260.455923	-2260.427983	17.5
		correction ^f	1.3

^a BP86-D3/def2-TZVP total energies from Turbomole calculations. ^b Energy calculations in gas phase for geometry optimized in gas phase; ^c Energy calculations in acetone (COSMO model, $\epsilon=21$) for geometry optimized in gas phase; ^d Energy calculations in gas phase for geometry optimized in acetone (COSMO model). ^e Energy calculations in acetone for geometry optimized in acetone (COSMO model, $\epsilon=21$). ^f Difference between ΔE values for solvated (acetone/acetone) and unsolvated (gas/gas) model, the values subtracted are boldfaced.

Details of COSMO calculations. Atomic radii (Å): Fe 2.223, O 1.72, N 1.83, C 2.00, H 1.30; rsolv 1.30 Å. Dielectric constant assumed: $\epsilon=80$ (water) or $\epsilon=21$ (acetone).

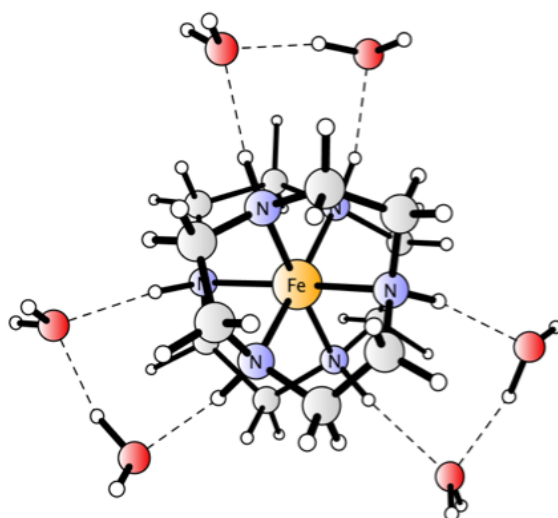


Figure S1: Optimized structure of complex **3** with six explicit water molecules (**3+6W**).

Table S5: Estimating Effects of Crystal Environment for Spin-State Energetics of **2**.

model ^a	Total energies (a.u.) ^b				ΔE (kcal/mol)	
	S=1/2	S=3/2		avg ^c	min ^d	
2 (gas) ^e (BP86-D3)	-0.534536	-0.519307	-0.517335	-0.517252	10.4	9.6
2 (gas) ^e	-0.534096	-0.519056	-0.516955	-0.517035	10.3	9.4
2 (crystal) ^f	-0.529413	-0.504953	-0.502808	-0.502726	16.3	15.3
2 (crystal) ^f + Ewald ^g	-2.128885	-2.105705	-2.103240	-2.103176	15.6	14.5
2(Cl)₉ (crystal) ^f	-0.326097	-0.303081	-0.300473	-0.300510	15.5	14.4
2(Cl)₉ (crystal) ^f + Ewald ^g	-3.725556	-3.702517	-3.700090	-3.700133	15.5	14.5
					correction ^h	6.0

^a All structures optimized at the PBE/pob-TZVP level except the first one marked “BP86-D3” optimized at the BP86-D3/def2-TZVP level; in all cases for the (1el)₃ isomer. ^b CASPT2(9e,12o) total energies shifted by +1841 a.u. for **2** or by +5991 a.u. for **2(Cl)₉**. ^c Average vertical excitation energy for three quasi-degenerate S=3/2 states (corresponding to one absorption band observed in experimental spectrum). ^d Vertical excitation energy to the lowest S=3/2 state. ^e (gas): geometry either for single gaseous ion. ^f (crystal): geometry of **3** or **2(Cl)₉**, taken from periodic DFT optimization of [Fe(en)₃]Cl₃. ^g including Ewald potential to simulate electrostatic field from the remaining ions in the lattice (ions replaced by point charges: +3 for **2** centered on Fe atom, -1 for Cl); the Ewald potential was simulated by including the array of point charges for 5x5x4 supercell and the quantum cluster (QC) chosen as either **2** or **2(Cl)₉**; 501 (QC **2**) or 492 (QC **2(Cl)₉**) charges lying within 23.25 Å from the central iron were fixed to their formal values, whereas the remaining charges were optimized to reproduce the Ewald potential at 1000 random check points within the QC. ^h Difference between ΔE (avg)^c for **2(Cl)₉** + Ewald and ΔE (min)^d for gaseous **2**, the values subtracted are boldfaced.

Table S6: DFT Spin-State Energetics for 1.

	$E(S=5/2)^a$ (a.u.)	$\langle S^2 \rangle$ ($S=5/2$)	$E(S=3/2^{QR})^a$ (a.u.)	$\langle S^2 \rangle^b$ ($S=3/2^{QR}$)	$E(S=3/2^{BS})^a$ (a.u.)	$\langle S^2 \rangle^c$ ($S=3/2^{BS}$)	ΔE_{rel}^b (kcal/mol)	$\Delta E_{\text{rel}}^{\text{BS}^d}$ (kcal/mol)	$\Delta E_{\text{rel}}^{\text{BSC}^e}$ (kcal/mol)	ΔE^{best^f} (kcal/mol)
BLYP	-1.500891	8.754	-1.462294	3.773	-1.462919	4.047	24.2	23.8	25.3	25.5
B1LYP	-1.369970	8.756	-1.312961	3.778	-1.314581	4.167	35.8	34.8	37.9	38.1
B3LYP	-1.565310	8.755	-1.512425	3.778	-1.513531	4.113	33.2	32.5	35.0	35.2
CAM-B3LYP	-1.452739	8.755	-1.396743	3.775	-1.397957	4.117	35.1	34.4	37.1	37.3
B3LYP*	-1.160847	8.755	-1.111344	3.777	-1.112172	4.077	31.1	30.5	32.7	32.8
B3LYP-45	-3.610927	8.756	-3.540519	3.773	-3.544121	4.296	44.2	41.9	47.1	47.2
O3LYP	-1.551165	8.755	-1.486706	3.792	-1.487499	4.089	40.4	40.0	42.9	43.0
OLYP	-1.663951	8.755	-1.605246	3.788	-1.605961	4.082	36.8	36.4	39.0	39.1
OPBE	-1.536776	8.754	-1.472701	3.794	-1.474677	4.230	40.2	39.0	43.1	43.3
M06L	-1.431729	8.757	-1.358353	3.794	-1.358706	4.006	46.0	45.8	48.3	48.5
M06	-1.276970	8.758	-1.196830	3.787	— ^g	— ^g	50.3	—	—	50.5
M11L	-1.496552	8.756	-1.473843	3.767	— ^g	— ^g	14.2	—	—	14.4
M11	-1.322470	8.753	-1.268477	3.768	— ^g	— ^g	33.9	—	—	34.1
MN15L	-1.175786	8.756	-1.075441	3.837	— ^g	— ^g	63.0	—	—	63.1
MN15	-1.436687	8.754	-1.391824	3.761	— ^g	— ^g	28.2	—	—	28.3
LC-wPBE	-1.082129	8.753	-1.027709	3.773	-1.030094	4.211	34.1	32.7	36.0	36.1
LC-wHPBE	-1.079458	8.753	-1.025027	3.773	-1.027415	4.211	34.2	32.7	36.0	36.1
LC-BLYP	-0.359941	8.754	-0.306755	3.768	-0.307615	4.060	33.4	32.8	35.0	35.2
B97D	-1.782865	8.755	-1.720697	3.796	-1.721253	4.059	39.0	38.7	41.2	41.4
wB97XD	-1.417238	8.755	-1.361661	3.773	-1.362422	4.058	34.9	34.4	36.7	36.8
PW6B95	-2.714775	8.755	-2.657419	3.779	-2.658226	4.072	36.0	35.5	37.9	38.1
BR89	-1.280273	8.755	-1.226887	3.780	-1.227129	3.957	33.5	33.3	34.8	35.0
TPSS	-1.593841	8.754	-1.551604	3.780	-1.554241	4.257	26.5	24.8	27.7	27.8
TPSSh	-1.521125	8.755	-1.471398	3.784	-1.474579	4.284	31.2	29.2	32.7	32.9
PBE	-0.799493	8.754	-0.754744	3.777	-0.756517	4.196	28.1	27.0	29.6	29.8
PBE0	-0.816383	8.755	-0.752304	3.784	-0.755713	4.290	40.2	38.1	42.7	42.8
B2PLYP	-1.154721	8.756	-1.089641	3.773	-1.089159	4.343	40.8	41.1	46.7	46.8
SSB-D	-2.408197	8.755	-2.341928	3.797	-2.344076	4.246	41.6	40.2	44.7	44.8
S12g	-2.339545	8.754	-2.281783	3.786	-2.283317	4.186	36.2	35.3	38.7	38.8
S12h	-3.407674	8.755	-3.338761	3.789	-3.341142	4.237	43.2	41.7	46.3	46.4
MVS	-2.817788	8.755	-2.728910	3.804	-2.731615	4.155	55.8	54.1	58.8	59.0
MVSh	-3.812297	8.755	-3.712238	3.803	-3.715938	4.182	62.8	60.5	66.2	66.3
LH14t-calPBE	-0.032737	8.754	0.022569	3.786	0.021352	4.132	34.7	33.9	36.7	36.9

^a Total energies shifted up by 1720 a.u. (Gaussian) or “bond energies” with respect to atomic fragment (ADF). ^b Superscript QR refers to “quasi-restricted” solution with negligible spin contamination and number of effectively unpaired electrons $N_u \sim 3$. ^c Superscript BS refers to broken-symmetry solution with larger spin contamination and $N_u \sim 3.5-4$. ^d Energy of BS solution not corrected for spin contamination. ^e Energy of BS solution with added correction for spin contamination. ^f Best estimate of the sextet - quartet splitting, i.e. using the quartet energy of BS solution corrected for spin contamination or energy of QR solution if the BS one cannot be found, plus relativistic correction. ^g For these functionals, the BS solution cannot be found (even with a BS initial guess) and the QR solution was found stable. ^h SCF could not be converged.

Table S7: DFT Spin-State Energetics for **2**.

	E (S=1/2) (a.u.)	$\langle S^2 \rangle$ (S=1/2)	E(S=3/2) (a.u.)	$\langle S^2 \rangle$ (S=3/2)	ΔE_{nrrel} (kcal/mol)	ΔE (kcal/mol)
BLYP	-1834.505374	0.768	-1834.458933	3.784	29.1	29.1
B1LYP	-1834.366145	0.792	-1834.337859	3.801	17.7	17.7
B3LYP	-1834.728864	0.783	-1834.697152	3.798	19.9	19.9
CAM-B3LYP	-1834.467967	0.783	-1834.439307	3.792	18.0	18.0
B3LYP*	-1834.194036	0.776	-1834.159003	3.794	22.0	22.0
B3LYP-45	-1837.432382	0.840	-1837.413881	3.804	11.6	11.6
O3LYP	-1834.636071	0.774	-1834.611048	3.813	15.7	15.7
OLYP	-1834.715071	0.769	-1834.682668	3.805	20.3	20.3
OPBE	-1834.675122	0.771	-1834.645919	3.811	18.3	18.3
M06L	-1834.568787	0.772	-1834.541285	3.820	17.3	17.3
M06	-1834.217312	0.842	-1834.204865	3.807	7.8	7.8
M11L	-1834.729635	0.830	-1834.653640	3.780	47.7	47.7
M11	-1834.282194	0.764	-1834.266398	3.785	9.9	9.9
MN15L	-1834.138556	0.796	-1834.132475	3.876	3.8	3.8
MN15	-1834.320403	1.075	-1834.294458	3.770	16.3	16.3
LC-wPBE	-1834.162695	0.780	-1834.133361	3.784	18.4	18.4
LC-wHPBE	-1834.159631	0.780	-1834.130311	3.784	18.4	18.4
LC-BLYP	-1832.838917	0.769	-1832.810320	3.780	17.9	17.9
B97D	-1834.823348	0.772	-1834.794038	3.816	18.4	18.4
wB97XD	-1834.559131	0.778	-1834.530047	3.790	18.3	18.2
PW6B95	-1836.077561	0.782	-1836.050423	3.803	17.0	17.0
BR89	-1834.412146	0.770	-1834.372404	3.797	24.9	24.9
TPSS	-1834.846812	0.803	-1834.799656	3.795	29.6	29.6
TPSSh	-1834.754835	0.819	-1834.715444	3.803	24.7	24.7
PBE	-1833.742098	0.771	-1833.699175	3.789	26.9	26.9
PBE0	-1833.786251	0.804	-1833.762417	3.809	15.0	14.9
B2PLYP	-1834.137937	0.859	-1834.107983	3.810	18.8	18.8
SSB-D	-6.634393	0.779	-6.607997	3.818	16.6	16.6
S12g	-6.484919	0.771	-6.452045	3.804	20.6	20.6
S12h	-8.173222	0.795	-8.153827	3.816	12.2	12.2
MVS	-7.235053	0.771	-7.221949	3.842	8.2	8.2
MVSh	-8.805177	0.798	-8.803069	3.857	1.3	1.3
LH14t-calPBE	-1832.912111	0.790	-1832.879855	3.806	20.2	20.2

Table S8: DFT Spin-State Energetics for **3**.

	E (S=0) (a.u.)	E (S=2) (a.u.)	$\langle S^2 \rangle$ (S=2)	ΔE_{rel} (kcal/mol)	ΔE (kcal/mol)
BLYP-D3	-2067.256195	-2067.234025	6.007	13.9	15.7
BLYP	-2067.157431	-2067.137618	6.007	12.4	14.3
B1LYP	-2067.015117	-2067.030157	6.007	-9.4	-7.6
B3LYP-D3	-2067.599579	-2067.604623	6.007	-3.2	-1.3
B3LYP	-2067.519402	-2067.525542	6.007	-3.9	-2.0
CAM-B3LYP-D3	-2067.198195	-2067.202633	6.006	-2.8	-1.0
CAM-B3LYP	-2067.142463	-2067.147703	6.006	-3.3	-1.5
B3LYP*-D3	-2066.902459	-2066.898587	6.007	2.4	4.3
B3LYP-45-D3	-2071.123275	-2071.166665	6.007	-27.2	-25.4
O3LYP	-2067.317177	-2067.335121	6.009	-11.3	-9.4
OLYP	-2067.372336	-2067.376925	6.010	-2.9	-1.0
OPBE	-2067.344454	-2067.346530	6.011	-1.3	0.5
M06L-D3	-2067.345146	-2067.344651	6.015	0.3	2.1
M06L	-2067.339929	-2067.339464	6.015	0.3	2.1
M06-D3	-2066.867332	-2066.887910	6.017	-12.9	-11.1
M06	-2066.853763	-2066.874285	6.017	-12.9	-11.0
M11L	-2067.513296	-2067.415146	6.011	61.6	63.4
M11	-2066.953431	-2066.984688	6.005	-19.6	-17.8
MN15L	-2066.748588	-2066.774072	6.039	-16.0	-14.2
MN15	-2066.852951	-2066.850579	6.009	1.5	3.3
LC-wPBE-D3	-2066.882168	-2066.882563	6.005	-0.2	1.6
LC-wPBE	-2066.823135	-2066.824354	6.005	-0.8	1.1
LC-wHPBE	-2066.819486	-2066.820746	6.005	-0.8	1.0
LC-BLYP	-2064.957205	-2064.951207	6.005	3.8	5.6
B97D	-2067.448828	-2067.446118	6.011	1.7	3.5
wB97XD	-2067.304665	-2067.306272	6.007	-1.0	0.8
PW6B95-D3	-2069.234692	-2069.235617	6.006	-0.6	1.3
PW6B95	-2069.196789	-2069.198336	6.006	-1.0	0.9
BR89	-2067.213842	-2067.211593	6.010	1.4	3.2
TPSS-D3	-2067.750057	-2067.720361	6.006	18.6	20.5
TPSS	-2067.682819	-2067.654249	6.006	17.9	19.8
TPSSh-D3	-2067.637330	-2067.624094	6.006	8.3	10.1
TPSSh	-2067.570092	-2067.557982	6.006	7.6	9.4
PBE-D3	-2066.271668	-2066.247192	6.007	15.4	17.2
PBE	-2066.223873	-2066.199949	6.007	15.0	16.8
PBE0-D3	-2066.359963	-2066.373676	6.007	-8.6	-6.8
PBE0	-2066.310055	-2066.324326	6.007	-9.0	-7.1
B2PLYP-D3	-2066.808232	-2066.810213	6.007	-1.2	0.6
B2PLYP	-2066.764824	-2066.767506	6.007	-1.7	0.1
SSB-D	-9.991701	-9.993004	6.011	-0.8	1.0
S12g	-9.772631	-9.771241	6.010	0.9	2.7
S12h	-11.995377	-12.022904	6.008	-17.3	-15.4
MVS	-10.770641	-10.774959	6.015	-2.7	-0.9
MVSh	-12.846424	-12.880437	6.012	-21.3	-19.5
LH14t-calPBE-D3	-2065.322758	-2065.323544	6.006	-0.5	1.3
LH14t-calPBE	-2065.271150	-2065.272595	6.006	-0.9	0.9

Table S9: DFT Spin-State Energetics for 4.

	E (S=1/2) (a.u.)	$\langle S^2 \rangle$ (S=1/2)	E (S=5/2) (a.u.)	$\langle S^2 \rangle$ (S=5/2)	ΔE_{nrrel} (kcal/mol)	ΔE (kcal/mol)
BLYP-D3	-2259.837023	0.764	-2259.815125	8.758	13.7	14.9
BLYP	-2259.753612	0.764	-2259.730161	8.758	14.7	15.9
B1LYP	-2259.545800	0.799	-2259.555928	8.762	-6.4	-5.2
B3LYP-D3	-2260.190295	0.784	-2260.193434	8.761	-2.0	-0.8
B3LYP	-2260.121418	0.784	-2260.123112	8.761	-1.1	0.1
CAM-B3LYP-D3	-2259.696100	0.788	-2259.698481	8.760	-1.5	-0.3
CAM-B3LYP	-2259.647722	0.788	-2259.649034	8.760	-0.8	0.3
B3LYP*-D3	-2259.388828	0.775	-2259.384090	8.761	3.0	4.1
B3LYP-45-D3	-2264.245322	0.875	-2264.283625	8.762	-24.0	-22.9
O3LYP	-2259.856299	0.770	-2259.871754	8.761	-9.7	-8.5
OLYP	-2259.941224	0.766	-2259.943402	8.760	-1.4	-0.2
OPBE	-2259.854660	0.769	-2259.854128	8.759	0.3	1.5
M06L-D3	-2259.928872	0.764	-2259.946413	8.763	-11.0	-9.9
M06L	-2259.923297	0.764	-2259.940878	8.763	-11.0	-9.9
M06-D3	-2259.335327	0.829	-2259.371290	8.764	-22.6	-21.4
M06	-2259.322239	0.829	-2259.358344	8.764	-22.7	-21.5
M11L	-2260.057539	0.799	-2259.967875	8.761	56.3	57.4
M11	-2259.446472	0.760	-2259.464129	8.758	-11.1	-9.9
MN15L	-2259.208117	0.789	-2259.265314	8.763	-35.9	-34.7
MN15	-2259.235609	1.051	-2259.225236	8.759	6.5	7.7
LC-wPBE-D3	-2259.291656	0.788	-2259.285830	8.758	3.7	4.8
LC-wPBE	-2259.240479	0.788	-2259.233541	8.758	4.4	5.5
LC-wHPBE	-2259.236389	0.788	-2259.229491	8.758	4.3	5.5
LC-BLYP	-2257.049900	0.771	-2257.038653	8.758	7.1	8.2
B97D	-2259.909504	0.768	-2259.916971	8.761	-4.7	-3.5
wB97XD	-2259.800325	0.781	-2259.802015	8.761	-1.1	0.1
PW6B95-D3	-2262.052754	0.784	-2262.056776	8.762	-2.5	-1.4
PW6B95	-2262.019668	0.784	-2262.022906	8.762	-2.0	-0.9
BR89	-2259.915465	0.769	-2259.915009	8.759	0.3	1.4
TPSS-D3	-2260.384312	0.795	-2260.353044	8.759	19.6	20.8
TPSS	-2260.326741	0.795	-2260.294589	8.759	20.2	21.3
TPSSh-D3	-2260.236179	0.822	-2260.219999	8.760	10.2	11.3
TPSSh	-2260.179727	0.822	-2260.162580	8.760	10.8	11.9
PBE-D3	-2258.671552	0.767	-2258.646182	8.758	15.9	17.1
PBE	-2258.629972	0.767	-2258.604112	8.758	16.2	17.4
PBE0-D3	-2258.727971	0.819	-2258.739375	8.761	-7.2	-6.0
PBE0	-2258.684429	0.819	-2258.695115	8.761	-6.7	-5.5
B2PLYP-D3	-2259.282814	0.905	-2259.284255	8.762	-0.9	0.3
B2PLYP	-2259.245426	0.905	-2259.245931	8.762	-0.3	0.8
SSB-D	-11.281522	0.774	-11.292016	8.760	-6.6	-5.4
S12g	-11.069244	0.767	-11.069113	8.759	0.1	1.2
S12h	-13.475389	0.804	-13.502405	8.761	-17.0	-15.8
MVS	-12.150212	0.771	-12.175118	8.761	-15.6	-14.5
MVSh	-14.402872	0.799	-14.456197	8.762	-33.5	-32.3
LH14-calPBE-D3	-2257.559967	0.791	-2257.556198	8.760	2.4	3.5
LH14-cal-PBE	-2257.515256	0.791	-2257.510927	8.760	2.7	3.9

Table S10: Nonrelativistic (nrel) and Relativistic (rel) DFT:B3LYP Spin-State Energetics for **1**.

	E (S=5/2) (a.u.)	$\langle S^2 \rangle$ (S=5/2)	E (S=3/2) (a.u.)	$\langle S^2 \rangle$ (S=3/2)	ΔE (kcal/mol)
B3LYP/cc-pVTZ (nrel)	-1721.513806	8.755	-1721.461421	3.778	32.9
B3LYP/cc-pVTZ-DK (rel)	-1730.749247	8.755	-1730.696589	3.776	33.0

Table S11: Nonrelativistic (nrel) and Relativistic (rel) DFT:B3LYP Spin-State Energetics for **2**.

	E (S=1/2) (a.u.)	$\langle S^2 \rangle$ (S=1/2)	E (S=3/2) (a.u.)	$\langle S^2 \rangle$ (S=3/2)	ΔE (kcal/mol)
B3LYP/cc-pVTZ (nrel)	-1834.695183	0.781	-1834.663065	3.797	20.2
B3LYP/cc-pVTZ-DK (rel)	-1843.883065	0.781	-1843.850959	3.795	20.1

Table S12: Nonrelativistic (nrel) and Relativistic (rel) DFT:B3LYP Spin-State Energetics for **3**.

	E (S=0) (a.u.)	E (S=2) (a.u.)	$\langle S^2 \rangle$ (S=2)	ΔE (kcal/mol)
B3LYP/cc-pVTZ (nrel)	-2067.478971	-2067.483984	6.007	-3.1
B3LYP/cc-pVTZ-DK (rel)	-2076.755033	-2076.757128	6.007	-1.3

Table S13: Nonrelativistic (nrel) and Relativistic (rel) DFT:B3LYP Spin-State Energetics for **4**.

	E (S=1/2) (a.u.)	$\langle S^2 \rangle$ (S=1/2)	E (S=5/2) (a.u.)	$\langle S^2 \rangle$ (S=5/2)	ΔE (kcal/mol)
B3LYP/cc-pVTZ (nrel)	-2260.070925	0.783	-2260.071324	8.761	-0.3
B3LYP/cc-pVTZ-DK (rel)	-2269.457025	0.782	-2269.455582	8.761	0.9

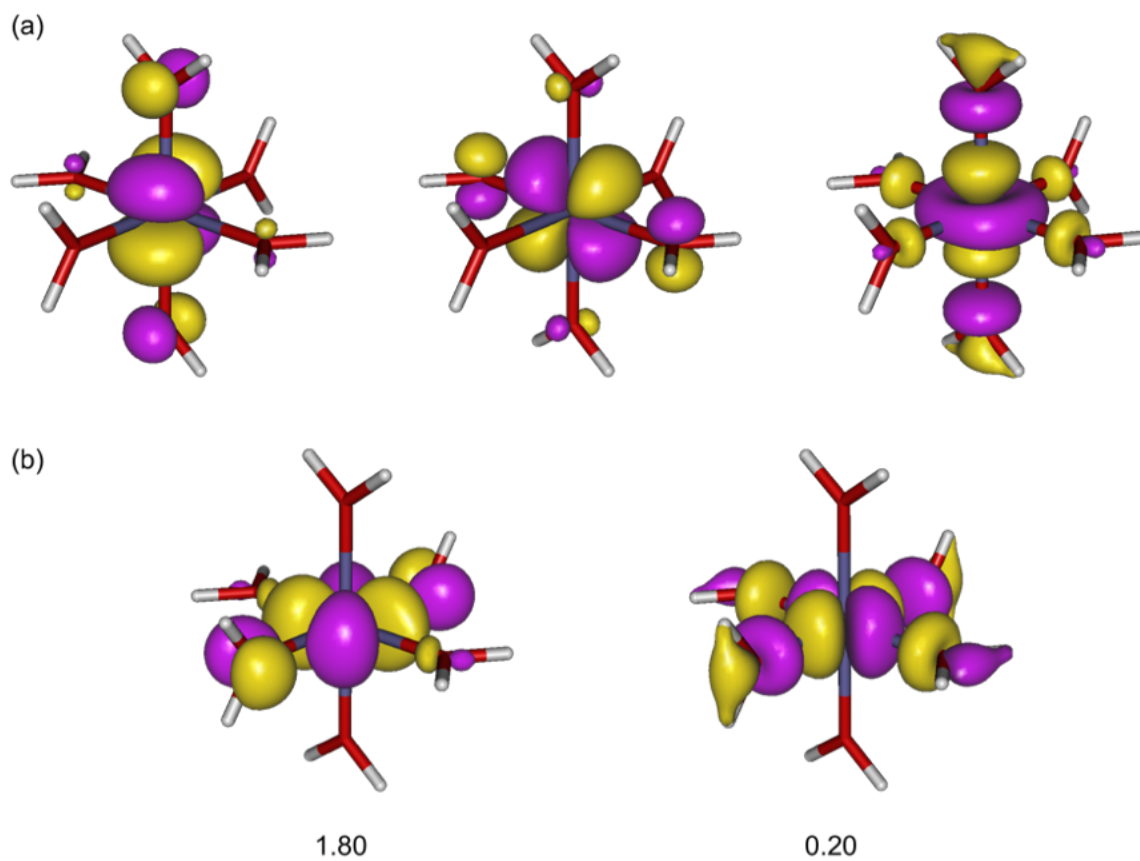


Figure S2: Contour plots of natural orbitals for BS quartet solution of complex **1** from B3LYP/def2-QZVPP calculation: (a) three singly occupied orbitals; (b) two fractionally occupied orbitals (with occupation numbers indicated); contour values ± 0.04 au.

Table S14: Basis Sets T(D)-DK and T(D), and Auxiliary Basis Sets for F12 Calculations.

	Fe	first sphere	remaining atoms
T(D)-DK	cc-pwCVTZ-DK ^a	cc-pVTZ-DK ^b	cc-pVDZ-DK ^b
T(D)	cc-pwCVTZ ^a	cc-pVTZ ^c	cc-pVDZ ^c
T(D),df_basis ^d	aug-cc-pVTZ/mp2fit ^e	aug-cc-pVTZ/mp2fit ^f	aug-cc-pVDZ/mp2fit ^f
T(D),df_basis_exch ^g	def2-TZVPP/jkfit ^h	aug-cc-pVTZ/jkfit ⁱ	aug-cc-pVDZ/jkfit ⁱ
T(D),ri_basis ^j	def2-TZVPP/jkfit ^h	aug-cc-pVTZ/optri ^k	aug-cc-pVDZ/optri ^k

^a ref S5; ^b ref S7; ^c ref S6; ^d basis set for density fitting; ^e ref S8; ^f ref S9; ^g density fitting basis for computing the exchange and Fock operators; ^h ref S10; ⁱ ref S11; ^j basis set for RI; ^k ref S12. See end of ESI for refs S5 - S12.

Table S15: Detailed Results of CC Calculations for **1**.

	E (S=5/2) (au)	E (S=3/2) (au)	ΔE (kcal/mol)
RCCSD(T)/T(D)-DK	-1729.246749	-1729.165648	50.9
RCCSD(T)/T(D)-DK frozen 3s3p	-1728.833921	-1728.746607	54.8
KS-RCCSD(T)/T(D)-DK	-1729.240928	-1729.161127	50.1
RCCSD(T)/T(D)	-1720.049510	-1719.968793	50.7
RCCSD(T)-F12a/T(D)	-1720.343929	-1720.266873	48.4
UCCSD(T)/T(D)-DK	-1729.248248	-1729.167753	50.5
UCCSD(T)/T(D)-DK frozen 3s3p	-1728.834701	-1728.748090	54.3
KS-UCCSD(T)/T(D)-DK	-1729.242838	-1729.163087	50.0
UCCSD(T)/T(D)	-1720.051113	-1719.971014	50.3
UCCSD(T)-F12a/T(D)	-1720.345620	-1720.269130	48.0
ROHF/T(D)-DK	-1727.074243	-1726.943087	82.3
(T)/T(D)-DK (from UCCSD(T))	-0.062129	-0.069118	-4.4

Table S16: Detailed Results of CC Calculations for **2**.

	E (S=1/2) (au)	E (S=3/2) (au)	ΔE (kcal/mol)
RCCSD(T)/T(D)-DK	-1841.747596	-1841.719062	17.9
RCCSD(T)/T(D)-DK frozen 3s3p	-1841.321601	-1841.295581	16.3
KS-RCCSD(T)/T(D)-DK	-1841.740052	-1841.710301	18.7
RCCSD(T)/T(D)	-1832.599026	-1832.570470	17.9
RCCSD(T)-F12a/T(D)	-1833.121220	-1833.089666	19.8
UCCSD(T)/T(D)-DK	-1841.748275	-1841.721990	16.5
UCCSD(T)/T(D)-DK frozen 3s3p	-1841.322138	-1841.298022	15.1
KS-UCCSD(T)/T(D)-DK	-1841.740608	-1841.712522	17.6
UCCSD(T)/T(D)	-1832.599724	-1832.573469	16.5
UCCSD(T)-F12a/T(D)	-1833.121877	-1833.092608	18.4
ROHF/T(D)-DK	-1838.664357	-1838.678332	-8.8
(T)/T(D)-DK (from UCCSD(T))	-0.121882	-0.114286	4.8

Table S17: Detailed Results of CC Calculations for **3**.

	E (S=0) (au)	E (S=2) (au)	ΔE (kcal/mol)
RCCSD(T)/T(D)-DK	-2073.936691	-2073.933589	1.9
RCCSD(T)/T(D)-DK frozen 3s3p	-2073.511396	-2073.512618	-0.8
KS-RCCSD(T)/T(D)-DK	-2073.921717	-2073.919766	1.2
RCCSD(T)/T(D)	-2064.702964	-2064.703342	-0.2
RCCSD(T)-F12a/T(D)	-2065.474164	-2065.466842	4.6
UCCSD(T)/T(D)-DK	-2073.936691	-2073.934803	1.2
UCCSD(T)/T(D)-DK frozen 3s3p	-2073.511396	-2073.513373	-1.2
KS-UCCSD(T)/T(D)-DK	-2073.921717	-2073.920802	0.6
UCCSD(T)/T(D)	-2064.702964	-2064.704558	-1.0
UCCSD(T)-F12a/T(D)	-2065.474164	-2065.468084	3.8
R(O)HF/T(D)-DK	-2069.916330	-2070.024589	-67.9
(T)/T(D)-DK (from UCCSD(T))	-0.157780	-0.140499	10.8

Table S18: Detailed Results of CC Calculations for **4** and **4'**.

	E (S=1/2) (au)	E (S=5/2) (au)	ΔE (kcal/mol)
4 UCCSD(T)/T(D)-DK	-2266.096587	-2266.103401	-4.3
4' UCCSD(T)/T(D)-DK	-2109.209579	-2109.213661	-2.6
UCCSD(T)/T(D)-DK frozen 3s3p	-2108.783441	-2108.795411	-7.5
KS-UCCSD(T)/T(D)-DK	-2109.201750	-2109.202679	-0.6
UCCSD(T)/T(D)	-2099.926593	-2099.932103	-3.5
UCCSD(T)-F12a/T(D)	-2100.681083	-2100.677354	2.3
RCCSD(T)/T(D)-DK	-2109.207589	-2109.209615	-1.3
RCCSD(T)/T(D)-DK frozen 3s3p	-2108.781964	-2108.792982	-6.9
KS-RCCSD(T)/T(D)-DK	- ^a	-2109.200626	-
RCCSD(T)/T(D)	-2099.924499	-2099.927783	-2.1
RCCSD(T)-F12a/T(D)	-2100.678862	-2100.672678	3.9
ROHF/T(D)-DK	-2105.269177	-2105.406688	-86.3
(T)/T(D)-DK (from UCCSD(T))	-0.178276	-0.156290	13.8

^a The CCSD iterations did not converge.

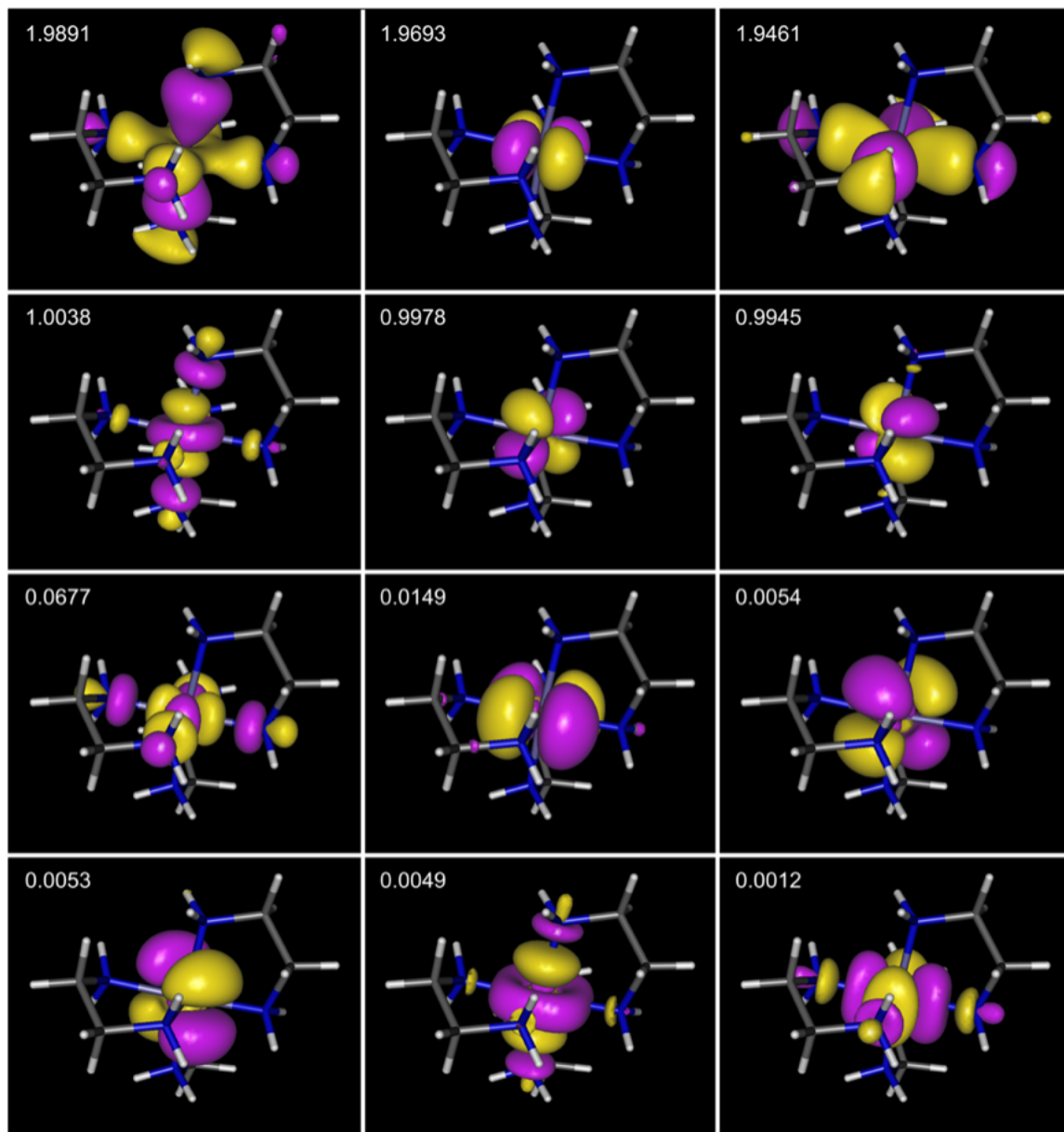
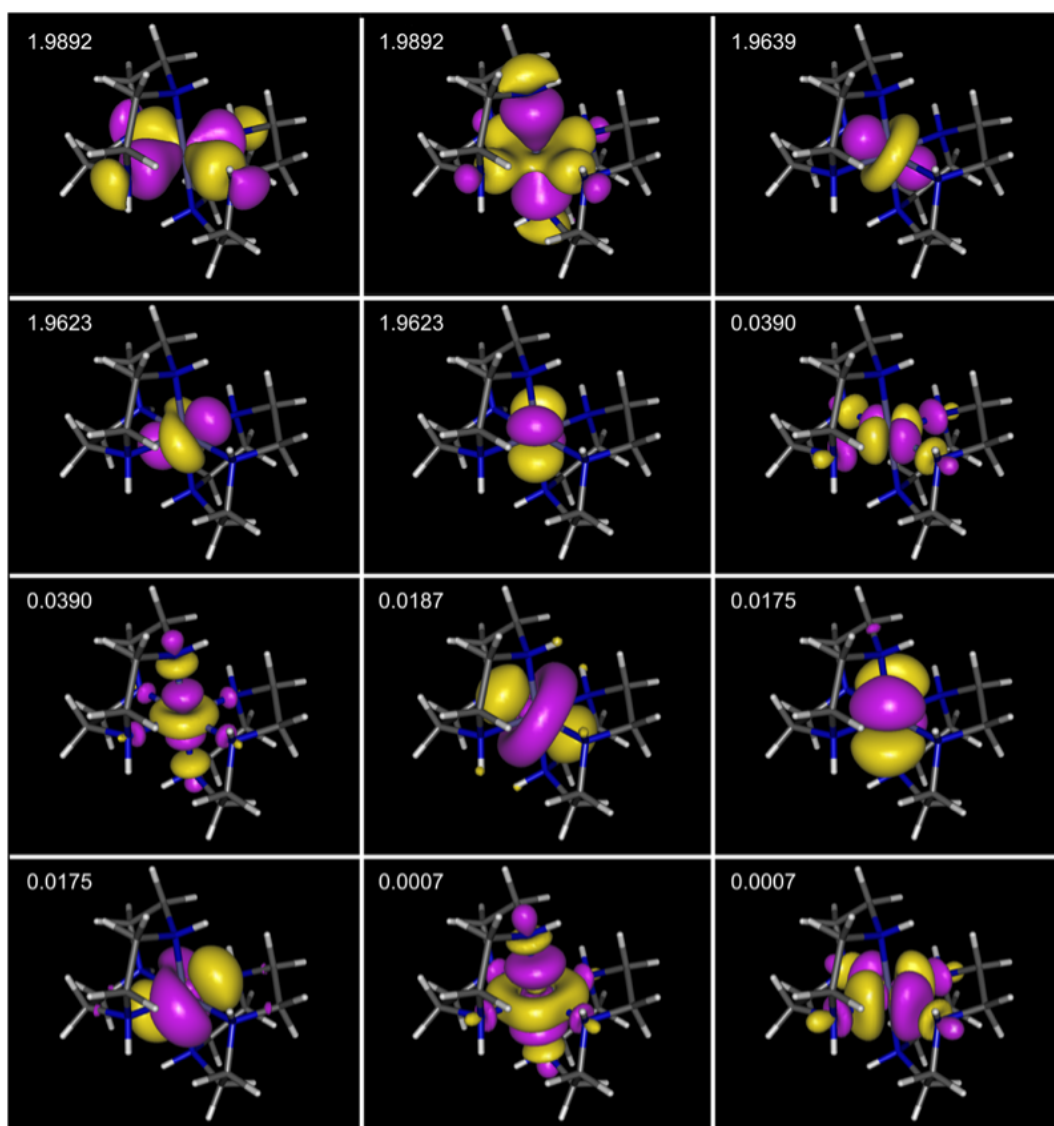


Figure S3: Contour plots of natural orbitals from CASSCF(9e,12o) calculations for the $S=3/2$ state of complex **2** with annotated occupation numbers. Contour values for all plots: ± 0.04 au.

(a)



(b)

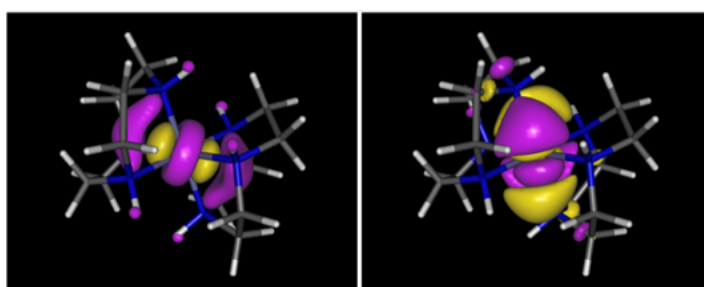
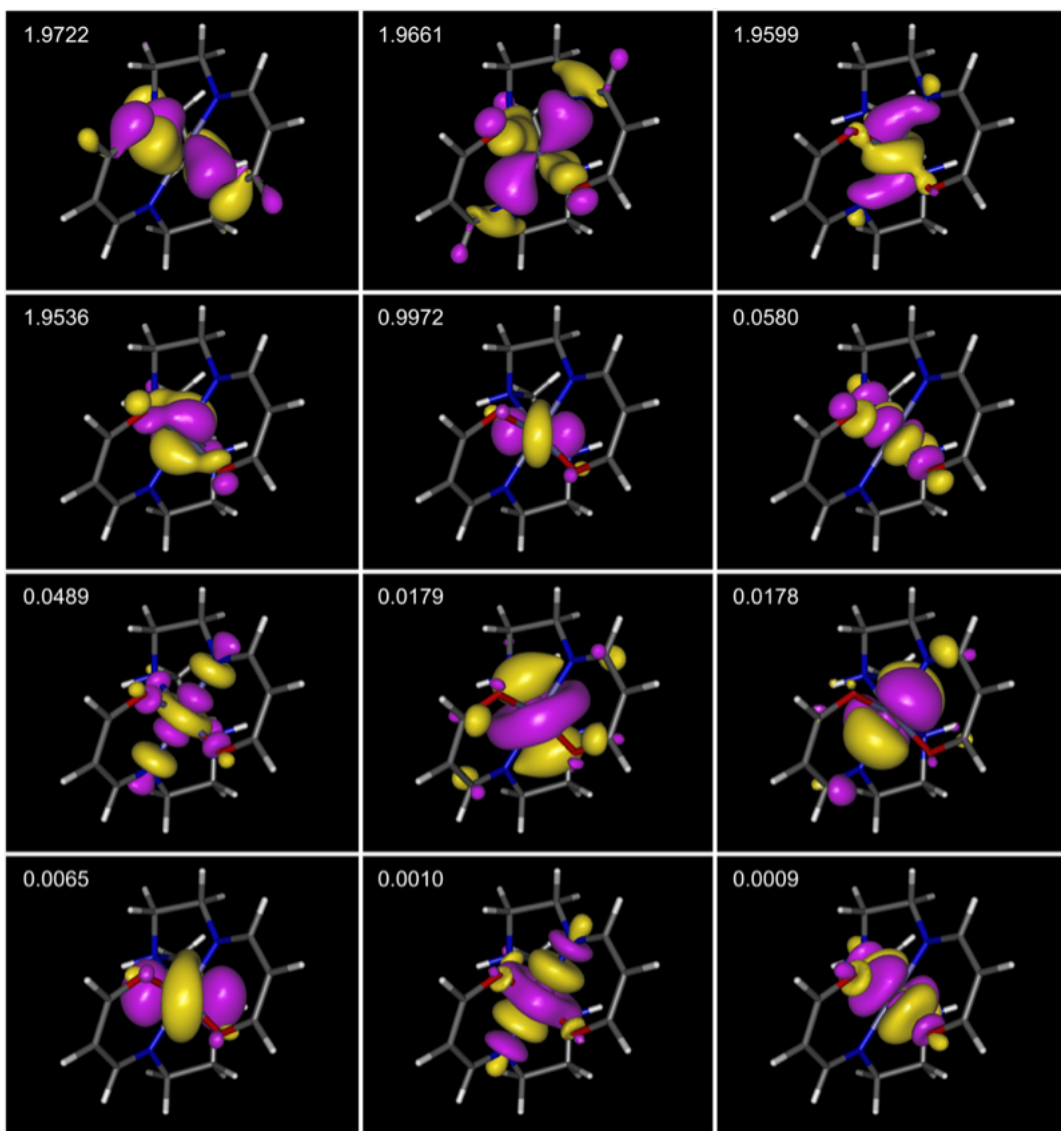


Figure S4: Contour plots of natural orbitals from CASSCF(10e,12o) calculations for the LS state of complex **3**: (a) The final 12 active orbitals with annotated natural occupation numbers, denoted below as (10e,12o) “correct”. (b) Two “unwanted” virtual orbitals which tend to replace the last two orbitals depicted in (a) during standard CASSCF(10e,12o) calculations in Molcas; the problem was circumvented by taking converged orbitals from Molpro. Contour values for all plots: +/- 0.04 au.

(a)



(b)

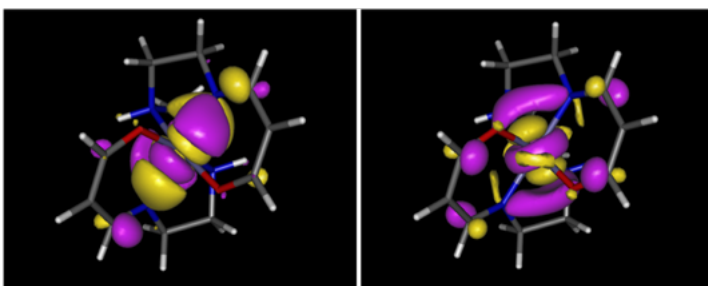


Figure S5: Contour plots of natural orbitals from CASSCF(9e,12o) calculations for the LS state of complex **4'**: (a) The final 12 active orbitals with annotated occupation numbers, denoted below as (9e,12o) “correct”. (b) Two “unwanted” virtual orbitals which tend to replace the last two orbitals depicted in (a) during standard CASSCF(9e,12o) calculations; the problem was circumvented by performing first CASSCF(9e,14o) calculations, after which the two “unwanted” orbitals were removed from the active space and constrained to remain virtual. Contour values for all plots: +/- 0.04 au.

Table S19: Detailed Results of Multi-Reference Calculations for **1**.^a

	E (S=5/2) (au)	E (S=3/2) (au) ^a	ΔE (kcal/mol)
CASPT2(9,12)	-1729.166542	-1729.078481	55.3
CASPT2(9,12) frozen 3s3p	-1728.751874	-1728.661239	56.9
pc-NEVPT2(9,12)	-1729.125649	-1729.052625	45.8
sc-NEVPT2(9,12)	-1729.116686	-1729.041055	47.5
MRCISD(9,12)	-1728.721007	-1728.628903	57.8
MRCISD+Q(9,12) (Davidson, fixed)	-1729.073174	-1728.988084	53.4
MRCISD+Q(9,12) (Davidson, relaxed)	-1729.072739	-1728.987483	53.5
MRCISD+Q(9,12) (Davidson-Silver, fixed)	-1729.171997	-1729.090113	51.4
MRCISD+Q(9,12) (Pople, fixed)	-1729.148303	-1729.065760	51.8
MRCISD+Q(9,12) (Meissner, fixed)	-1729.050273	-1728.964727	53.7
C_0 (fixed) ^c	0.90568225	0.90490474	
C_0 (relaxed) ^c	0.90578270	0.90504200	

^a All calculations performed with the T(D)-DK basis set. ^b Three degenerate components of the 4T_g term were optimized together in state-average CASSCF(9e,12o) calculations (three lowest A_g roots in C_i point group used in Molcas; or lowest B_{1g} , B_{2g} , B_{3g} roots in D_{2h} point group used in Molpro). ^c Coefficient of the reference function.

The size-consistency corrections for MRCISD are defined as follows (see refs 90-93, main article):

$$\Delta E_D = \Delta E_c \times \frac{1 - C_0^2}{C_0^2} \quad (S1)$$

$$\Delta E_{DS} = \Delta E_c \times \frac{1 - C_0^2}{2C_0^2 - 1} \quad (S2)$$

$$\Delta E_P = \Delta E_c \times \left(\frac{\sqrt{N_e^2 + 2N_e \tan^2(2 \cos^{-1} C_0)} - N_e}{2(\sec(2 \cos^{-1} C_0) - 1)} - 1 \right) \quad (S3)$$

$$\Delta E_M = \Delta E_D \frac{(N_e - 3)(N_e - 2)}{N_e(N_e - 1)} \quad (S4)$$

where N_e is the number of correlated electrons, C_0 is the coefficient of reference function, ΔE_c is the dynamic correlation energy resulting from MRCISD.

Table S20: Detailed Results of Multi-Reference Calculations for **2**. ^a

	E (S=1/2) (au)	E (S=3/2) (au)	ΔE (kcal/mol)
CASPT2(9,12)	-1841.534536	-1841.514390	12.6
CASPT2(9,12) frozen 3s3p	-1841.114815	-1841.091673	14.5
pc-NEVPT2(9,12)	-1841.516884	-1841.485521	19.7
sc-NEVPT2(9,12)	-1841.501482	-1841.471008	19.1
MRCISD(9,12)	-1840.722180	-1840.702944	12.1
MRCISD+Q(9,12) (Davidson, fixed)	-1841.323860	-1841.301431	14.1
MRCISD+Q(9,12) (Davidson, relaxed)	-1841.323215	-1841.300862	14.0
MRCISD+Q(9,12) (Davidson-Silver, fixed)	-1841.594842	-1841.570058	15.6
MRCISD+Q(9,12) (Pople, fixed)	-1841.555615	-1841.531158	15.3
MRCISD+Q(9,12) (Meissner, fixed)	-1841.297560	-1841.275270	14.0
C ₀ (fixed) ^b	0.873529	0.873773	
C ₀ (relaxed) ^b	0.873640	0.873871	

^a All calculations performed with the T(D)-DK basis set. ^b Coefficient of the reference function.

Table S21: Detailed Results of Multi-Reference Calculations for **3**.^a

	E (S=0) (au)	E (S=2) (au)	ΔE (kcal/mol)
CASPT2(10,12)	-2073.634879	-2073.643260	-5.3
CASPT2(10,12) frozen 3s3p	-2073.217738	-2073.220363	-1.6
pc-NEVPT2(10,12)	-2073.614810	-2073.604828	6.3
sc-NEVPT2(10,12)	-2073.604294	-2073.598011	3.9
MRCISD(10,12)	-2072.370539	-2072.399580	-18.2
MRCISD+Q(10,12) (Davidson, fixed)	-2073.215458	-2073.231195	-9.9
MRCISD+Q(10,12) (Davidson, relaxed)	-2073.214887	-2073.230855	-10.0
MRCISD+Q(10,12) (Davidson-Silver, fixed)	-2073.696183	-2073.701375	-3.3
MRCISD+Q(10,12) (Pople, fixed)	-2073.644198	-2073.650545	-4.0
MRCISD+Q(10,12) (Meissner, fixed)	-2073.187870	-2073.204041	-10.1
C ₀ (fixed) ^b	0.856663	0.857122	
C ₀ (relaxed) ^b	0.856740	0.857168	

^a All calculations performed with the T(D)-DK basis set. ^b Coefficient of the reference function.

Table S22: Detailed Results of Multi-Reference Calculations for **4** and **4'**.^a

		E (S=1/2) (au)	E (S=5/2) (au)	ΔE (kcal/mol)
4'	CASPT2(9,12)	-2108.958432	-2108.963307	-3.1
	CASPT2(9,12) frozen 3s3p	-2108.537184	-2108.543601	-4.0

4	CASPT2(9,12)	-2265.776757	-2265.784247	-4.7
	CASPT2(9,12) frozen 3s3p	-2265.355561	-2265.364154	-5.4
	pc-NEVPT2(9,12)	-2265.719283	-2265.730844	-7.3
	sc-NEVPT2(9,12)	-2265.701964	-2265.717622	-9.8
	MRCISD(9,12)	-2264.175858	-2264.212436	-23.0
	MRCISD+Q(9,12) (Davidson, fixed)	-2265.157043	-2265.179036	-13.8
	MRCISD+Q(9,12) (Davidson, relaxed)	-2265.156395	-2265.178584	-13.9
	MRCISD+Q(9,12) (Davidson-Silver, fixed)	-2265.767899	-2265.778792	-6.8
	MRCISD+Q(9,12) (Pople, fixed)	-2265.709282	-2265.721263	-7.5
	MRCISD+Q(9,12) (Meissner, fixed)	-2265.128909	-2265.151321	-14.1
	C ₀ (fixed) ^b	0.850120	0.850364	
	C ₀ (relaxed) ^b	0.850198	0.850419	

^a All calculations performed with the T(D)-DK basis set. ^b Coefficient of the reference function.

Table S23: Variations of CASSCF and CASPT2 Energies for LS State (2A) of **4'** Caused by Problematic Double-Shell Orbitals ^a

	CASSCF		CASPT2	
	(total, au)	(relative to "correct", kcal/mol)	(total, au)	(relative to "correct", kcal/mol)
(9e,12o) "correct"	-2105.381192	0	-2108.958432	0
(9e,12o) "unwanted"	-2105.384886	-2.3	-2108.955159	2.1
(9e,10o)	-2105.376695	2.8	-2108.952946	3.4

^a For additional explanation, see Figure S4 and main article.

Table S24: Variations of CASSCF and CASPT2 Energies for LS State (1A) of **3** Caused by Problematic Double-Shell Orbitals ^a

	CASSCF		CASPT2	
	(total, au)	(relative to "correct", kcal/mol)	(total, au)	(relative to "correct", kcal/mol)
(10e,12o) "correct"	-2070.040561	0	-2073.634879	0
(10e,12o) "unwanted"	-2070.044139	-2.2	-2073.635895	-0.6
(10e,10o)	-2070.036509	2.5	-2073.633710	0.7

^a For additional explanation, see Figure S4 and main article.

Table S25: Best Estimates of Relative Spin-State Energetics from WFT Methods ^a

	1	2	3	4^b
RCCSD(T) ^c	-48.6	19.8	6.8	3.0
UCCSD(T) ^c	-48.2	18.4	6.0	1.5
KS-UCCSD(T) ^d	-47.8	19.5	5.4	3.5
CASPT2 ^e	-53.0	14.5	-0.4	1.1
pc-NEVPT2 ^e	-43.6	21.6	11.1	-1.5
sc-NEVPT2 ^e	-45.2	21.0	8.8	-4.0
MRCISD ^e	-55.5	14.0	-13.4	-17.2
MRCISD+Q(D) ^{e,f}	-51.1	16.0	-5.1	-8.0
MRCISD+Q(DS) ^{e,f}	-49.1	17.4	1.6	-1.0
MRCISD+Q(P) ^{e,f}	-49.5	17.2	0.8	-1.7
MRCISD+Q(M) ^{e,f}	-51.4	15.9	-5.3	-8.3
CASPT2/CC ^g	-50.8	17.8	5.6	5.1

^a All values are relative energies defined as $E(S_2)-E(S_1)$ in kcal/mol. ^b Part of CC calculations were performed for smaller model 4' and corrected for the model effect of -1.7 kcal/mol estimated at the UCCSD(T)/T(D) level; see Table S22. ^c Calculated from eq. (2), main article. ^d Calculated from eq. (4), main article. ^e Calculated from eq. (5), main article. ^f size-consistency corrections: D = Davidson, DS = Davidson-Silver, P = Pople, M = Meissner; all using fixed reference coefficient, calculated from eq. (S1)-(S4) on page S18. ^g Calculated from eq. (6), main article.

Table S26: Signed Errors of WFT Methods with Respect to Reference Data of Spin-State Energetics for Complexes **1-4** and Mean Signed Error (MSE), Mean Absolute Error (MAE), and Maximum Error (MAX) for Each Method.^a

	1	2	3	4	MSE	MAE	MAX
RCCSD(T)	-1.2	0.1	3.0	0.6	0.6	1.2	3.0
UCCSD(T)	-0.8	-1.3	2.2	-0.9	-0.2	1.3	2.2
KS-UCCSD(T)	-0.4	-0.2	1.6	1.1	0.5	0.8	1.6
CASPT2	-5.6	-5.2	-4.2	-1.3	-4.1	4.1	5.6
pc-NEVPT2	3.8	1.9	7.3	-3.9	2.3	4.2	7.3
sc-NEVPT2	2.2	1.3	5.0	-6.4	0.5	3.7	6.4
MRCISD	-8.1	-5.7	-17.2	-19.6	-12.7	12.7	19.6
MRCISD+Q(D)	-3.7	-3.7	-8.9	-10.4	-6.7	6.7	10.4
MRCISD+Q(DS)	-1.7	-2.3	-2.2	-3.4	-2.4	2.4	3.4
MRCISD+Q(P)	-2.1	-2.5	-3.0	-4.1	-2.9	2.9	4.1
MRCISD+Q(M)	-4.0	-3.8	-9.1	-10.7	-6.9	6.9	10.7
CASPT2/CC	-3.4	-1.9	1.8	2.7	-0.2	2.4	3.4

^a All values in kcal/mol.

Table S27: Diagnostics of Multireference Character. ^a

		1	2	3	4'
T ₁	S ₁	0.023	0.026	0.019	0.030
	S ₂	0.019	0.023	0.012	0.025
D ₁	S ₁	0.129	0.155	0.110	0.158
	S ₂	0.063	0.174	0.056	0.122
T ₁ ^{KS}	S ₁	0.017	0.010	0.011	0.011
	S ₂	0.020	0.011	0.011	0.015
D ₁ ^{KS}	S ₁	0.068	0.033	0.036	0.042
	S ₂	0.072	0.042	0.046	0.066
spin contamination	S ₁	0.014	0.007	0.000	0.007
	S ₂	0.001	0.017	0.001	0.002
spin contamination (KS)	S ₁	0.01244	0.00862	0.00000	0.00686
	S ₂	0.00174	0.01602	0.00109	0.00181
%MC ^b	S ₁	5.60%	8.10%	6.46%	7.89%
	S ₂	0.80%	6.61%	1.75%	1.10%
M ^c	S ₁	0.0636	0.0529	0.0389	0.0536
	S ₂	0.0074	0.0666	0.0216	0.0087
B (kcal/mol) ^d		12.6	11.4	21.9	21.1

^a T₁, D₁, and spin contamination are reported at the UCCSD/T(D)-DK level. ^b The %MC diagnostics (percentage multi configurational character) is defined as $1 - C_0^2$, where C_0 is the CI coefficient of the principal configuration appearing in a CASSCF wave function expanded using natural orbitals optimized for each state. ^c The M diagnostics is calculated from occupation numbers of natural CASSCF orbitals in Table S28. ^d The B diagnostics is calculated as the difference between the ΔE_e values from BLYP and B1LYP calculations from Tables S6-S9.

Table S28: Natural Orbital Occupation Numbers from CASSCF/T(D)-DK Calculations.

1		2		3		4'	
S ₁	S ₂						
1.99611	1.99859	1.96786	1.98911	1.98953	1.99876	1.97217	1.99713
1.98210	1.99859	1.96785	1.96930	1.98952	1.99863	1.96608	1.99654
1.94409	0.99864	1.95663	1.94608	1.96350	1.98568	1.95992	0.99985
0.99977	0.99864	1.95662	1.00379	1.96182	0.99712	1.95360	0.99940
0.99677	0.99733	0.99570	0.99777	1.96182	0.99698	0.99724	0.99686
0.99608	0.99733	0.05810	0.99447	0.03959	0.99555	0.05806	0.99681
0.06384	0.99733	0.05808	0.06770	0.03957	0.99532	0.04888	0.99678
0.00922	0.00267	0.01521	0.01486	0.01865	0.01380	0.01793	0.00359
0.00385	0.00267	0.01521	0.00544	0.01743	0.00481	0.01775	0.00347
0.00385	0.00267	0.00647	0.00534	0.01743	0.00477	0.00647	0.00323
0.00371	0.00276	0.00114	0.00491	0.00058	0.00433	0.00097	0.00320
0.00062	0.00276	0.00114	0.00122	0.00058	0.00427	0.00092	0.00315

Complete references 74, 75, 78, 80, 84, and 89

[74] R. Dovesi, V. R. Saunders, C. Roetti, R. Orlando, C. M. Zicovich-Wilson, F. Pascale, B. Civalleri, K. Doll, N. M. Harrison, I. J. Bush, P. D'Arco, M. Llunell, M. Causà and Y. Noël, *CRYSTAL14 User's Manual*, University of Torino, 2014.

[75] R. Dovesi, R. Orlando, A. Erba, C. M. Zicovich-Wilson, B. Civalleri, S. Casassa, L. Maschio, M. Ferrabone, M. De La Pierre, P. D'Arco, Y. Noël, M. Causà, M. Rérat and B. Kirtman, *Int. J. Quantum Chem.*, 2014, **114**, 1287–1317.

[78] E. J. Baerends, T. Ziegler, A. J. Atkins, J. Autschbach, D. Bashford, O. Baseggio, A. Bérces, F. M. Bickelhaupt, C. Bo, P. M. Boerritger, L. Cavallo, C. Daul, D. P. Chong, D. V. Chulhai, L. Deng, R. M. Dickson, J. M. Dieterich, D. E. Ellis, M. van Faassen, A. Ghysels, A. Giammona, S. J. A. van Gisbergen, A. Goetz, A. W. Götz, S. Gusarov, F. E. Harris, P. van den Hoek, Z. Hu, C. R. Jacob, H. Jacobsen, L. Jensen, L. Joubert, J. W. Kaminski, G. van Kessel, C. König, F. Kootstra, A. Kovalenko, M. Krykunov, E. van Lenthe, D. A. McCormack, A. Michalak, M. Mitoraj, S. M. Morton, J. Neugebauer, V. P. Nicu, L. Noodleman, V. P. Osinga, S. Patchkovskii, M. Pavanello, C. A. Peebles, P. H. T. Philipsen, D. Post, C. C. Pye, H. Ramanantoanina, P. Ramos, W. Ravenek, J. I. Rodríguez, P. Ros, R. Rüger, P. R. T. Schipper, D. Schlüns, H. van Schoot, G. Schreckenbach, J. S. Seldenthuis, M. Seth, J. G. Snijders, M. Solà, S. M., M. Swart, D. Swerhone, G. te Velde, V. Tognetti, P. Vernooijs, L. Versluis, L. Visscher, O. Visser, F. Wang, T. A. Wesolowski, E. M. van Wezenbeek, G. Wiesenekker, S. K. Wolff, T. K. Woo and A. L. Yakovlev, *ADF2017*, SCM, Theoretical Chemistry, Vrije Universiteit, Amsterdam, The Netherlands, <https://www.scm.com>.

[80] M. J. Frisch, G. W. Trucks, H. B. Schlegel, G. E. Scuseria, M. A. Robb, J. R. Cheeseman, G. Scalmani, V. Barone, G. A. Petersson, H. Nakatsuji, X. Li, M. Caricato, A. V. Marenich, J. Bloino, B. G. Janesko, R. Gomperts, B. Mennucci, H. P. Hratchian, J. V. Ortiz, A. F. Izmaylov, J. L. Sonnenberg, D. Williams-Young, F. Ding, F. Lipparini, F. Egidi, J. Goings, B. Peng, A. Petrone, T. Henderson, D. Ranasinghe, V. G. Zakrzewski, J. Gao, N. Rega, G. Zheng, W. Liang, M. Hada, M. Ehara, K. Toyota, R. Fukuda, J. Hasegawa, M. Ishida, T. Nakajima, Y. Honda, O. Kitao, H. Nakai, T. Vreven, K. Throssell, J. A. Montgomery, Jr., J. E. Peralta, F. Ogliaro, M. J. Bearpark, J. J. Heyd, E. N. Brothers, K. N. Kudin, V. N. Staroverov, T. A. Keith, R. Kobayashi, J. Normand, K. Raghavachari, A. P. Rendell, J. C. Burant, S. S. Iyengar, J. Tomasi, M. Cossi, J. M. Millam, M. Klene, C. Adamo, R. Cammi, J. W. Ochterski, R. L. Martin, K. Morokuma, O. Farkas, J. B. Foresman and D. J. Fox, *Gaussian 16 Revision B.01*, 2016, Gaussian Inc. Wallingford CT.

[84] H.-J. Werner, P. J. Knowles, G. Knizia, F. R. Manby, M. Schütz, P. Celani, W. Györffy, D. Kats, T. Korona, R. Lindh, A. Mitrushenkov, G. Rauhut, K. R. Shamasundar, T. B. Adler, R. D. Amos, A. Bernhardsson, A. Berning, D. L. Cooper, M. J. O. Deegan, A. J. Dobbyn, F. Eckert, E. Goll, C. Hampel, A. Hesselmann, G. Hetzer, T. Hrenar, G. Jansen, C. Köppl, Y. Liu, A. W. Lloyd, R. A. Mata, A. J. May, S. J. McNicholas, W. Meyer, M. E. Mura, A. Nicklass, D. P. O'Neill, P. Palmieri, D. Peng, K. Pflüger, R. Pitzer, M. Reiher, T. Shiozaki, H. Stoll, A. J. Stone, R. Tarroni, T. Thorsteinsson and M. Wang, MOLPRO, versions 2012 and 2015, a package of ab initio programs, see <http://www.molpro.net>.

[89] F. Aquilante, J. Autschbach, R. K. Carlson, L. F. Chibotaru, M. G. Delcey, L. De Vico, I. Fdez. Galván, N. Ferré, L. M. Frutos, L. Gagliardi, M. Garavelli, A. Giussani, C. E. Hoyer, G. Li Manni, H. Lischka, D. Ma, P. ÅMalmqvist, T. Müller, A. Nenov, M. Olivucci, T. B. Pedersen, D. Peng, F. Plasser, B. Pritchard, M. Reiher, I. Rivalta, I. Schapiro, J. Segarra-Martí, M. Stenrup, D. G. Truhlar, L. Ungur, A. Valentini, S. Vancoillie, V. Veryazov, V. P. Vysotskiy, O. Weingart, F. Zapata and R. Lindh, *J. Comp. Chem.*, 2016, **37**, 506–541.

Additional references to the basis sets and auxiliary basis sets

def2-TZVP, def2-TZVPP, def2-QZVPP

[S1] F. Weigend, M. Häser, H. Patzelt and R. Ahlrichs *Chem. Phys. Lett.*, 1998, **294**, 143-152.

[S2] F. Weigend, F. Furche, R. Ahlrichs, *J. Chem. Phys.*, 2003, **119**, 12753-12762

[S3] F. Weigend, R. Ahlrichs, *Phys. Chem. Chem. Phys.*, 2005, **7**, 3297-3305.

STO TZ2P, TZ2P+

[S4] E. Van Lenthe and E. J. Baerends, *J. Comp. Chem.*, 2003, **24**, 1142-1156

cc-pwCVTZ, cc-pwCVTZ-DK for Fe

[S5] N.B. Balabanov, and K.A. Peterson, *J. Chem. Phys.*, 2006, **125**, 074110.

cc-pVTZ, cc-pVDZ

[S6] T.H. Dunning, *J. Chem. Phys.*, 1989, **90**, 1007-1023.

cc-pVTZ-DK, cc-pVDZ-DK

[S7] W.A. de Jong, R.J. Harrison, and D.A. Dixon, *J. Chem. Phys.*, 2001, **114**, 48-53.

aug-cc-pVTZ/mp2fit for Fe

[S8] J. G. Hill and J. A. Platts, *J. Chem. Phys.*, 2008, **128**, 044104.

aug-cc-pVTZ/mpf2fit for main-group elements

[S9] F. Weigend, A. Köhn, C. Hättig, *J. Chem. Phys.*, 2002, **116**, 3175-3183.

def2-TZVPP/jkfit for Fe

[S10] F. Weigend, *J. Comp. Chem.* 2008, **29**, 167-175

aug-cc-pVTZ/jkfit for main-group elements

[S11] F. Weigend, *Phys. Chem. Chem. Phys.* 2002, **4**, 4285-4291.

aug-cc-pVTZ/optri for main-group elements

[S12] K.E. Yousaf and K.A. Peterson, *Chem. Phys. Lett.* 2009, **476**, 303-307.